Electronic Interactions in Saturated and Unsaturated [1.1.1]-, [2.1.1]-, [2.2.1]-, and [2.2.2]Triblattanes – PE-Spectroscopic Investigations

Rolf Gleiter*[a], Christoph Sigwart[a], Wolf-Dieter Fessner[b], Hermann Müller-Bötticher[b], Horst Prinzbach*[b]

Organisch-Chemisches Institut der Universität Heidelberg[a],
Im Neuenheimer Feld 270, D-69120 Heidelberg

Chemisches Laboratorium der Universität Freiburg i.Br.[b],
Institut für Organische Chemie und Biochemie, Albertstr. 21, D-79104 Freiburg i. Br.

Received May 12, 1993

Key Words: Triblattanes / PE / Orbital sequence / Calculations

The He(I)-PE spectra of the parent [1.1.1]-, [2.1.1]-, [2.2.1]-, and [2.2.2]triblattanes **1**–**4**, of their unsaturated or ketonic congeners **5**–**13** and benzo derivatives **14**–**20** have been recorded. For **1**–**4**, the energy difference between the highest occupied orbitals (e″ and a′ mainly localized at the central bicyclo[2.2.2]octane unit) and the subsequent MOs increases with increasing number of ethano bridges. This observation is rationalized by using a first-order perturbation-theoretical approach. The analysis of the PE spectra of the *exo*-methylene (**5**–**7**), ketone (**8**–**10**), and *endo*-olefinic derivatives (**11**–**13**) unveils a strong π/σ mixing. The splitting of the π-bands in **7** (0.95 eV) and **13** (1.0 eV), respectively, is traced back to a stronger π/σ mixing of the e MOs as compared to the a_2 MOs. An analogous interaction causes the splitting of the first bands of the ketones **8**–**10** (0.45 – 1.49 eV). For the benzo derivatives **14**–**20** the split of the π-bands is relatively small (0.35 – 0.7 eV).

Orbitals of nonconjugated π-systems can interact with each other by a "through-space" (OITS) and/or "through-bond" mode (OITB)[1]. The OITS mode is sometimes subdivided into the terms "homoconjugation"[2] and "spiroconjugation"[3]. A prerequisite common to all of these OITS types is the spatially confined proximity and orientation of the nonconjugated π-fragments[4] which can be achieved by their imbedding into a suitable σ-system. In fact, record OITS values (2.2 eV) approaching that of classical π,π conjugation have been recorded for D_{2h}-bissecododecahedradienes[5], in which the specific carbon skeleton enforces unusually short transanular π,π distances of 2.6 – 2.7 Å. In the OITB[6] mode the σ-framework participates in the conjugation and therefore is responsible for long-range interactions. Both OITS and OITB modes are important for the understanding of electron- and energy-transfer processes[7].

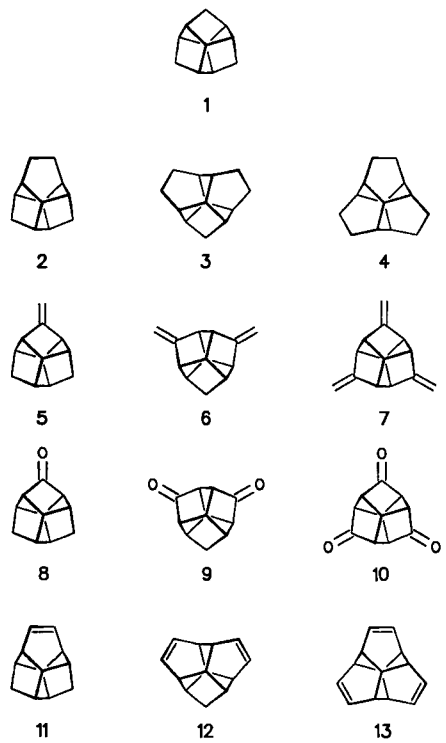

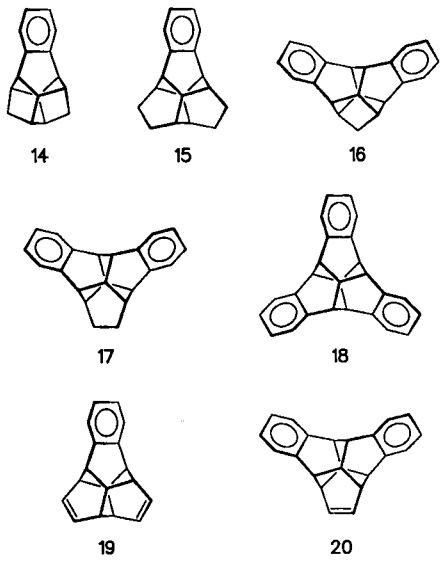

For a further evaluation of the interplay of OITS and OITB interactions between various chromophoric units within a novel, structurally defined environment, the recently synthesized rigid [1.1.1]-, [2.1.1]-, [2.2.1]-, and [2.2.2]triblattanes (**1**–**4**) together with their *exo*-methylene (**5**–**7**), ketone (**8**–**10**), olefinic (**11**–**13**), and benzoannulated derivatives (**14**–**20**) promised to be an attractive set of probes[8–11]. Particular interest was attached to the degree of "homoconjugation" in a D_3-symmetrical *cis,cis,cis*-cyclododeca-1,5,9-triene moiety in **13** (formally a cyclic, Moebius-type perimeter) which originally had been considered as precursors of novel $(CH)_{14}$ valence isomers[8,11].

In this paper we discuss the results of our He(I) photoelectron-(PE-)spectroscopical studies of the degree of π/π and π/σ interaction in these compounds.

Results and Discussion

For an interpretation of the PES results, the measured energy differences between the ground state of a molecule and the various ionic states have to be connected with the sequence of the valence electrons in the ground state. For a closed-shell molecule, to a good approximation the vertical ionization energies, $I_{v,j}$, can be set equal to the negative value, $-\varepsilon_j$, of the occupied canonical molecular orbitals (MOs): $I_{v,j} = -\varepsilon_j$. This result is generally referred to as Koopmans' theorem[12]. To derive the energies of the occupied MOs, we make use of semiempirical methods such as Dewar's MNDO procedure[13] which has proven to be quite reliable for the prediction of geometries and orbital sequence of hydrocarbons. Since the geometrical parameters of **1**–**17**, **19** and **20** were unknown, these were calculated by the MNDO procedure. A comparison with the X-ray structure of compound **18**[9] confirmed the reliability of this approach.

A) Photoelectron Spectra of [1.1.1]-, [2.1.1]-, [2.2.1]-, and [2.2.2]Triblattanes

The PE spectra of **2**–**4** are shown in Figure 1, the recorded vertical ionization energies for the first bands are collected in Table 1.

Table 1. Comparison between the recorded vertical ionization energies, $I_{v,j}$, and the calculated orbital energies, ε_j, of **1**–**4**, all values in eV

Compound	Band	$I_{v,j}$	Assignment	$-\varepsilon_j$ (MNDO/2)
1	1	9.9	$6a_1$	11.39
	2	10.25	9e	11.42
	3	10.45	8e	11.78
2	1	9.3	17a	11.0
	2	9.4	15b	11.21
	3	9.7	16a	11.28
	4	10.5	15a	11.62
3	1	9.06	17b	10.92
	2	9.2	18a	11.02
	3	9.5	17a	11.07
	4	10.45	16b	11.62
4	1	8.57	12e	10.86
	2	8.71		
	3	9.27	$8a_1$	10.96
	4	10.25	11e	11.86

Given the structural similarity of these hydrocarbons, the spectral discrepancies are at first sight somewhat surprising. While the PE spectrum of **1** shows only broad bands, an increase of vibrational fine structure with increasing number of ethano bridges is observed.

For a discussion of the shape and energies for the valence orbitals of **1**–**4** we start with the valence orbitals of bicyclo-[2.2.2]octane (**21**). The PE spectrum of this compound[14] starts with a peak at ca. 10 eV clearly separated from the

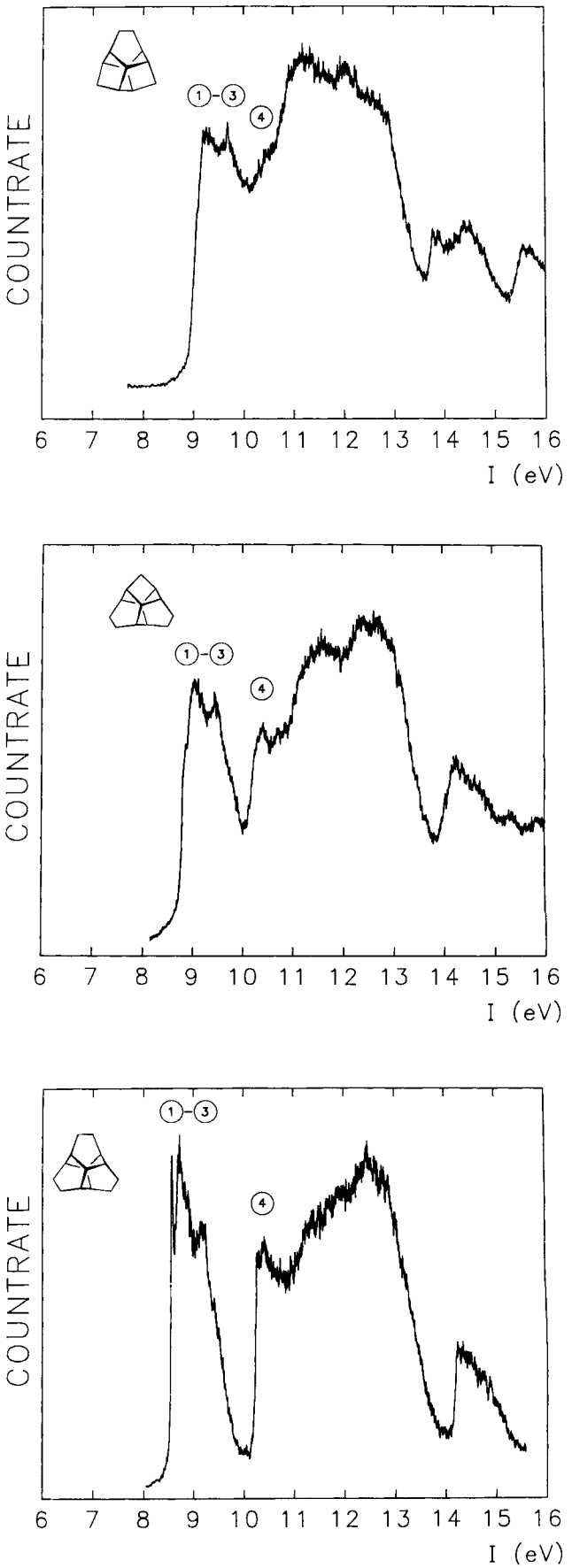

Figure 1. He(I)-PE spectra of **2**–**4**

higher energy region, a situation which is quite similar to that found for **2**–**4**. This peak is assigned to three ionization events, 3e″ and 4a′. The corresponding MOs are depicted schematically in Figure 2. They can be correlated with the ribbon orbitals of cyclohexane[15] and with the highest occupied MOs of **1**–**4**; therefore, we will refer to them as "ribbon orbitals" in the following discussion.

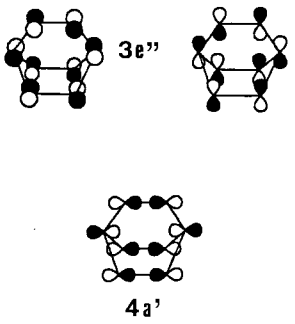

Figure 2. Schematic drawing of the highest occupied MOs of bicyclo[2.2.2]octane

Although in **1**–**4** the central bicyclo[2.2.2]octane unit is twisted by ca. 30–40°, the MO calculations indicate that the 3e″ and 4a′ combinations are hardly affected by this distortion. To derive **1**–**4** from **21** we proceed in two steps. First, we attach three or six methyl groups, respectively, to **21** in such a manner that at least C_3 symmetry is preserved (see **22** and **23**), then we connect the CH_3 groups in **22** to the skeleton to mimick **1**, whereas in **23** we form an ethano bridge from each pair of opposing CH_3 groups to generate **4**.

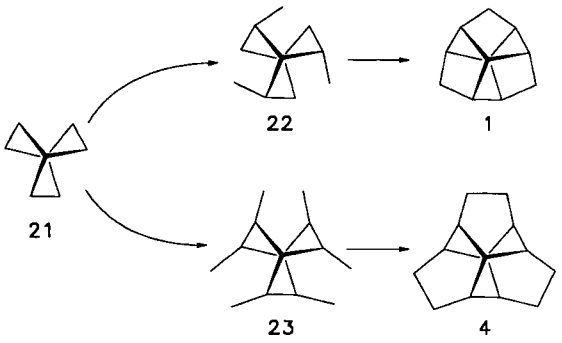

In Figure 3 the highest occupied MOs are illustrated for these models as derived from MNDO calculations. The calculations reproduce the PE data in that there is only a small energy gap between the two highest occupied MOs and the rest in the case of **1**, but a large gap in the case of **4**.

To rationalize this discrepancy, we consider the e MO of **21** and **22** at the carbon centers 2 and 8 in conjunction with a p orbital at the carbon center of the CH_3 groups (see below). If we bridge C-2 and C-8 with one CH_2 group, an additional bonding interaction arises which stabilizes the e levels. If both CH_3 groups at C-2 and C-8 in **23** form an ethano bridge, an additional antibonding interaction arises which destabilizes the e levels relative to **21**.

As a corollary of this rationalization it follows that we should expect high-lying PE bands for all [*m.n.p*]triblattanes

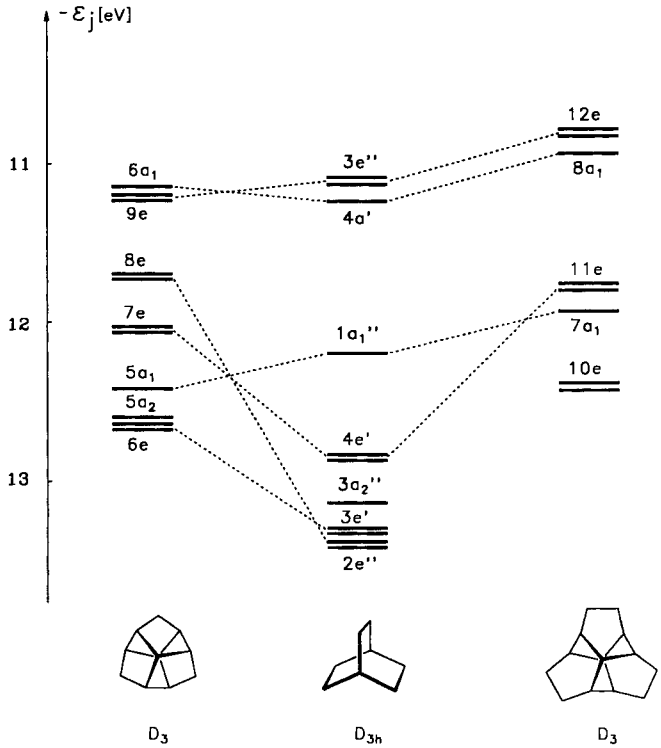

Figure 3. Comparison of the highest occupied MOs of bicyclo[2.2.2]octane (center) with those of [1.1.1]triblattane (left) and [2.2.2]triblattane (right); the values are derived from an MNDO/2 calculation

with *m*, *n*, and *p* being an even number. This model is supported by calculations performed on [3.3.3]- and [4.4.4]-triblattanes[16].

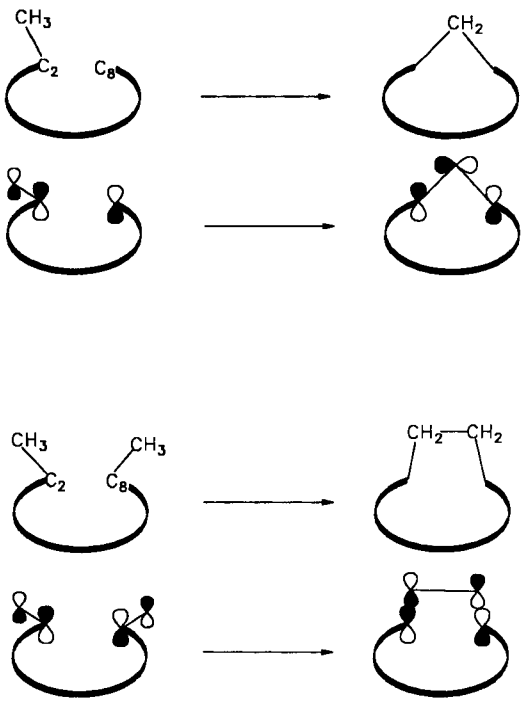

In Table 1 the recorded ionization energies are compared with the calculated orbital energies of **1**–**4**. Obviously, the

measured gap between the ribbon-type and the remaining orbitals in **2**–**4** is reproduced reasonably well.

B) Photoelectron Spectra of [1.1.1]Triblattanes with Exocyclic Double Bonds

1) *exo-Methylene Groups*

A common feature of the PE spectra of **5**–**7** (Figure 4, Table 2) are bands with a steep onset at lower ionization energy and a vibrational fine structure which is typical of ionization processes from π-MOs. The comparison of the PE characteristics with those of other *exo*-methylene compounds such as methylenecyclohexane ($I_{v,j} = 9.13$ eV[17]) and 2-methylenebicyclo[2.2.1]heptane ($I_{v,j} = 9.04$ eV[17]) supports the argument that the low-energy bands of **5**–**7** should be assigned to ionizations from π-MOs. The vibrational fine structure of the first band in the PE spectra of **5** and **6** ($\tilde{\nu} = 1210\ cm^{-1}$) compares well with those reported for other monoenes and dienes[14–17]. The energy difference between the first two bands of **6** and **7** amounts to 0.5 eV and 0.95 eV, respectively. As expected from the comparison with other simple π-systems we observe a shift of the first σ-bands to higher energies with increasing number of *exo*-methylene groups.

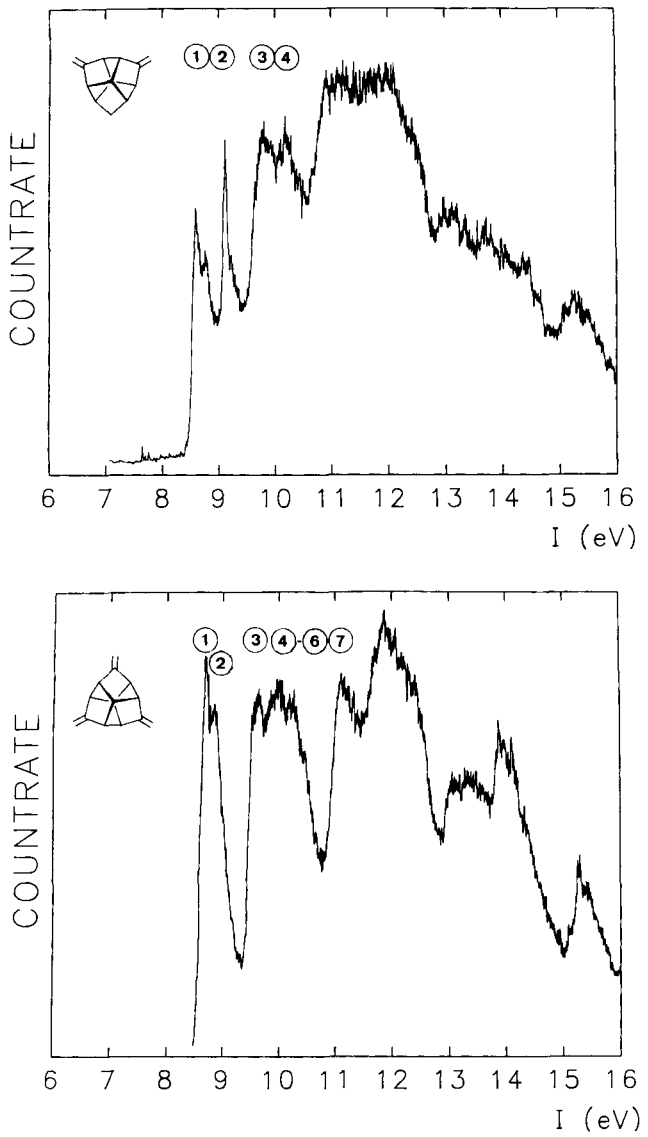

Figure 4. He(I)-PE spectra of **6** and **7**

Table 2. Comparison between the recorded vertical ionization energies, $I_{v,j}$, and the calculated orbital energies, ε_j, of **5**–**7**, all values in eV

Compound	Band	$I_{v,j}$	Assignment[a]	$-\varepsilon_j$ (MNDO/2)
5	1	8.90	15a(π)	9.77
	2	9.75	14b(σ_r)	11.34
6	1	8.67	17a(π)	9.63
	2	9.18	16b(π)	9.96
	3	9.9	16a(σ_r)	11.29
	4	10.3	15b(σ_r)	11.37
7	1, 2	8.73	11e(π)	9.63
	3	9.68	6a_2(π)	10.21
	4, 5	10.0_5	10e(σ_r)	11.29
	6	10.2	7a_1(σ_r)	11.41
	7	11.1_5	9e(σ)	12.02

[a] σ_r = σ-MO mainly centered at the triblattane skeleton ("ribbon" orbital).

Our empirical assignment is fully confirmed by MNDO calculations which imply a further splitting between the π-MOs of **6** and of **7** due to through-bond interaction[6]. For **7** a schematic drawing of the highest occupied MOs (11e and 6a_2) is given in Figure 5. The considerable split between 11e and 6a_2 points to a much stronger interaction of the e-linear combination of the three isolated π-bonds (right side of Figure 6) with the 8e-linear combination of the [1.1.1]triblattane fragment (left side of Figure 6) than with the a_2-linear combination of the π-bonds. The latter interacts with 4a_2. As can be seen from Figure 6, the energy difference e(π) – 8e(σ) amounts to ca. 1.8 eV and the difference a_2(π) – 4a_2(σ) to 2.8 eV. Therefore, according to first-order perturbation theory[18], the e(π)-e(σ) interaction should be much stronger than the a_2(π)-a_2(σ) interaction.

A similar analysis of the π/σ interactions in **6** again reveals that the splitting of the π-MOs in this compound is caused by their interaction with the σ-frame.

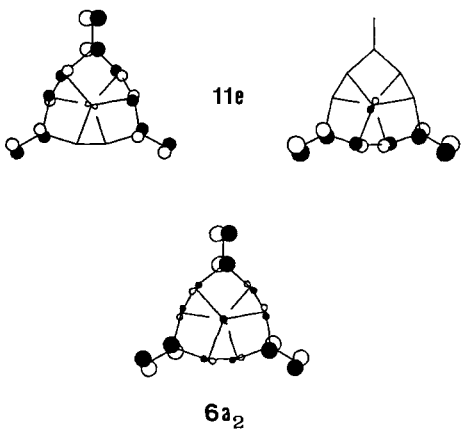

Figure 5. Schematic drawing of the highest occupied MOs of **7**

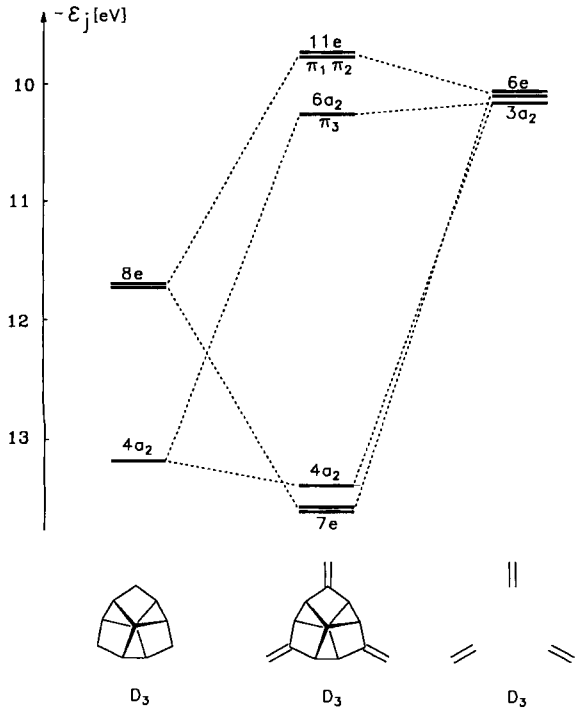

Figure 6. Interaction diagram between three ethylene fragments (right) and a [1.1.1]triblattane fragment (left) to yield the MOs of **7**; the values are derived from an MNDO/2 calculation

2) *Keto Groups*

In the PE spectra of the ketones **8**–**10** (Figure 7, Table 3) we find at low energies one (**8**) and two (**9**, **10**) peaks that are well separated from the other strongly overlapping bands. In the case of **10**, the ratio under the area of the first two peaks is approximately 2:1. The assignment of these bands is straightforward: They are due to the ionization of the 2p lone pair of the oxygen atom(s). Due to the high symmetry (D_3) of **10**, the first peak is assigned to the ionization from the 11e-linear combination. The first onset of the σ-bands is markedly shifted towards higher ionization energy with an increasing number of CO groups: **8**: 10.25 eV, **9**: 10.95 eV, and **10**: 11.40 eV.

Table 3. Comparison between the recorded vertical ionization energies, $I_{v,j}$, and the calculated orbital energies, ε_j, of **8**–**10**, all values in eV

Compound	Band	$I_{v,j}$	Assignment[a]	$-\varepsilon_j$ (MNDO/2)
8	1	8.76	15b(n)	10.30
	2	10.25	16a(σ_r)	11.76
9	1	9.0	17a(n)	10.43
	2	9.45	16b(n)	10.82
	3	10.95	16a(σ_r)	12.20
10	1	9.36	11e(n)	10.72
	2	9.50		
	3	10.26	6a_2(n)	11.41
	4	11.40	7a_1(σ_r)	12.58
	5	12.20	10e(σ_r)	12.96

[a] σ_r = σ-MO mainly centered at the triblattane skeleton ("ribbon" orbital).

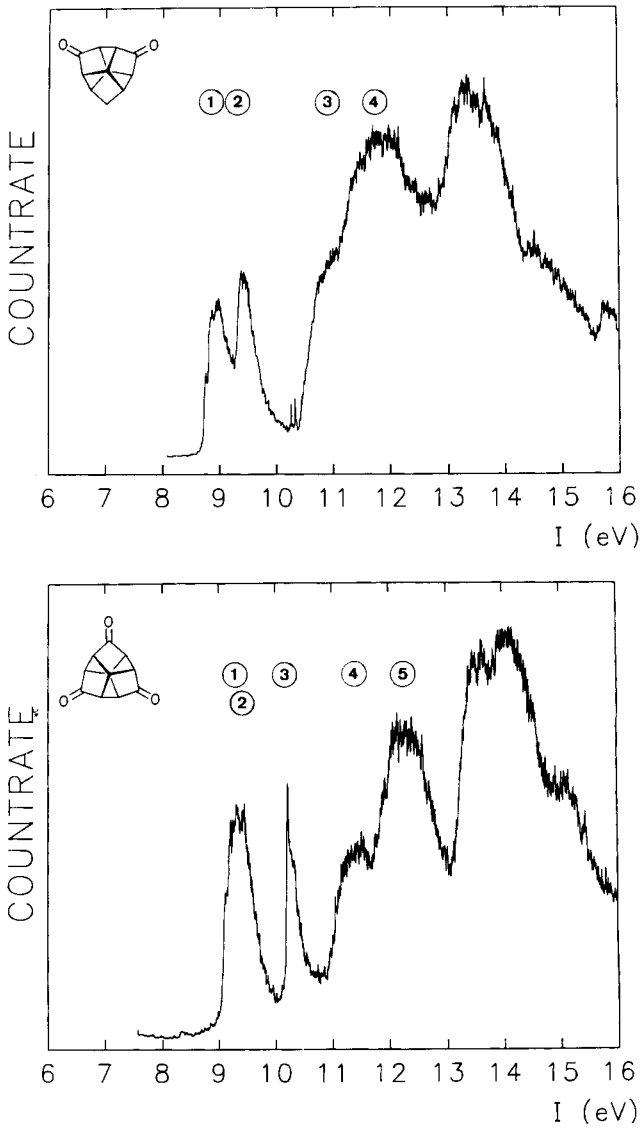

Figure 7. He(I)-PE spectra of **9** and **10**

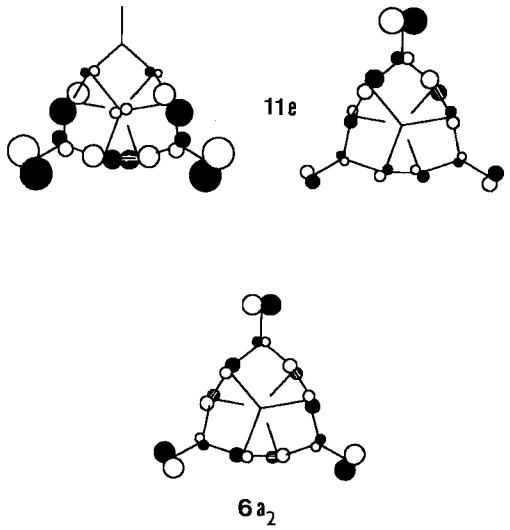

Figure 8. Schematic drawing of the highest occupied MOs of **10**

A comparison with the ionization energies of simple ketones (cyclohexanone: $I_{v,1} = 9.14$ eV[19]) or 1,4-diketones (cyclohexane-1,4-dione: $I_{v,1} = 9.65$ eV, $I_{v,2} = 9.80$ eV[20]; 1,5-dimethylbicyclo[3.3.0]octane-3,7-dione: $I_{v,1} = 9.31$ eV, $I_{v,2} = 9.58$ eV[21]) confirms our assignment which is corroborated by MNDO/2 calculations (Table 2). The predicted split of the n-orbitals for **9** and **10** comes close to the experimental one. Figure 8 displays the highest occupied MOs of **10** (11e and $6a_2$). A strong interaction between the 2p orbitals at the three oxygen centers and the σ-frame is evident.

C) Photoelectron Spectra of Triblattanes with Endocyclic Double Bonds

An analysis of the PE spectra of the olefins **11**–**13** (Figure 9, Table 4) can be derived from those of the parent compounds **2**–**4** which are formally related by replacement of the ethano bridges by C=C bonds. Such an exchange should increase the energy of the highest occupied σ-MO by 0.2–0.4 eV. This estimate stems from a comparison of the first σ-onset in the PE spectra of bicyclo[2.2.2]octene ($I_{v,2} = 10.03$ eV[14]) with the first ionization energy in bicyclo[2.2.2]octane ($I_{v,1} = 9.71$ eV[14]), cyclohexene ($I_{v,2} = 10.66$ eV[14]) and cyclohexane ($I_{v,1} = 10.32$ eV[14]).

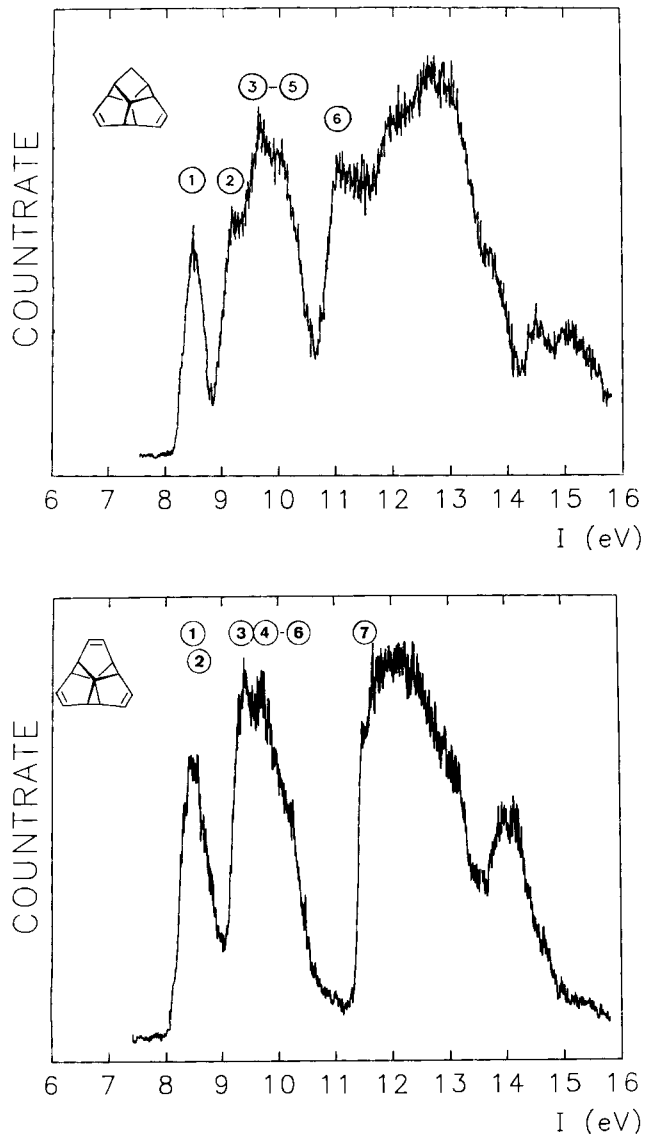

Figure 9. He(I)-PE spectra of **12** and **13**

Table 4. Comparison between the recorded vertical ionization energies, $I_{v,j}$, and the calculated orbital energies, ε_j, of **11**–**13**, all values in eV

Compound	Band	$I_{v,j}$	Assignment[a]	$-\varepsilon_j$ (MNDO/2)
11	1	8.70	15b(π)	9.65
	2	9.66	16a(σ_r)	11.25
	3	10.18	14b(σ_r)	11.27
12	1	8.4	17a(π)	10.43
	2	9.1	16b(π)	10.82
	3	9.5	16a(σ_r)	12.20
	4		15b(σ_r)	12.43
	5	10.0	15a(σ_r)	12.53
	6	11.0	14b(σ)	12.58
13	1, 2	8.5	11e(π)	9.51
	3	9.5	$6a_2$(π)	10.13
	4, 5	9.8	10e(σ_r)	11.03
	6	10.3	$7a_1$(σ_r)	11.42
	7	11.7	9e(σ)	12.74

[a] σ_r = σ-MO mainly centered at the triblattane skeleton ("ribbon" orbital).

On this basis we expect the first ionization energies to correspond to the ribbon orbital energies of **11** at 9.6 eV, of **12** at 9.7 eV, and of **13** at 9.7 eV. With this estimate for the first σ-ionizations we are left to attribute the first band in the PE spectrum of **11** and the first two peaks in the PE spectra of **12** and **13** to ionization events from π-MOs. The results of MO calculations listed in Table 4 are herewith in agreement. The measured splitting of the π-MOs in **12** (0.7 eV) and **13** (1.0 eV) documents a significant π/σ interaction which is represented by the 11e- and $6a_2$-combinations of **13** in Figure 10. Obviously, the π/σ interaction in 11e is stronger than in $6a_2$, a situation quite similar to that encountered for **7** and **10**.

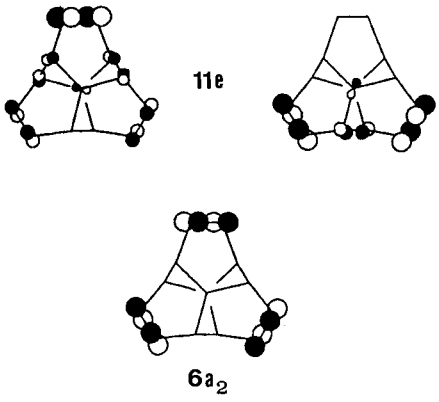

Figure 10. Schematic drawing of the highest occupied MOs of **13**

D) Photoelectron Spectra of Benzotriblattanes

As a start into this section, the benzotriblattanes **14**–**17** lacking additional double bonds will be considered initially.

The first bands in the PE spectra of **14** and **15** can be interpreted by a first-order treatment as a superposition of the first PE bands of an *o*-dialkylbenzene such as *o*-xylene[22], and those of **2** and **4**. Thus, the first two bands in both spectra at ca. 8.5 eV are identified as π-MOs from the benzene "e_S" and "e_A" MOs. In case of **15** these bands are located close to the bands arising from the ribbon orbitals (21b, 23a, 22a), while the π-bands of **14** are well separated from strongly overlapping σ-bands.

Table 5. Comparison between the recorded vertical ionization energies, $I_{v,j}$, and the calculated orbital energies, ε_j, of **14–18**, all values in eV

Compound	Band	$I_{v,j}$	Assignment[a]	$-\varepsilon_j$ (MNDO/2)
14	1	8.3	19b(π)	9.11
	2	8.7	21a(π)	9.26
	3	9.6	20a(σ_r)	11.16
15	1	8.25	22b(π)	9.16
	2	8.6	24a(π)	9.32
	3	9.1	21b(σ_r)	10.94
	4	9.4	23a(σ_r)	10.96
	5	9.6	22a(σ_r)	11.16
	6	10.5	20b(π)	11.82
16	1	8.1	26a(π)	9.06
	2	8.6	25b(π)	9.24
	3		25a(π)	9.31
	4		24b(π)	9.40
	5	9.6	24a(σ_r)	11.22
	6	9.9	23b(σ_r)	11.24
	7	10.1	23a(σ_r)	11.60
17	1	8.15	28a(π)	9.06
	2	8.7	26b(π)	9.25
	3		27a(π)	9.32
	4		25b(π)	9.41
	5	9.3	26a(σ_r)	11.02
	6	9.6	24b(σ_r)	11.10
	7	9.8	25a(σ_r)	11.34
	8	10.8	24a(σ)	11.87
18	1	8.1	20e(π)	9.06
	2			
	3	8.8	12a_1(π)	9.29
	4		10a_2(π)	9.41
	5		19e(π)	9.42
	6			
	7	9.5 to 10.3	18e(σ_r)	11.18
	8		11a_1(σ_r)	11.54
	9			
	10	11.0	17e(σ)	12.00

[a] σ_r = σ-MO mainly centered at the triblattane skeleton ("ribbon" orbital).

The PE spectra of **16–18** can be interpreted analogously. Due to the π-MOs of the benzene rings we expect four (**16**, **17**) and six (**18**) bands at the low-energy part, followed by the ionization of the ribbon orbitals of **3** and **4**. Indeed, this closely correlates with experiment (see Table 5, Figure 11), and MO calculations (MNDO/2) fully confirm the qualitative arguments (Table 5). Due to the high symmetry of **18** (D_3), the 12a(π) MO is a linear combination of only e_A fragments while 10a_2(π) is composed only of the e_S fragment. The linear combinations 20e(π) and 19e(π) of **18** entail both types of benzene π-orbitals.

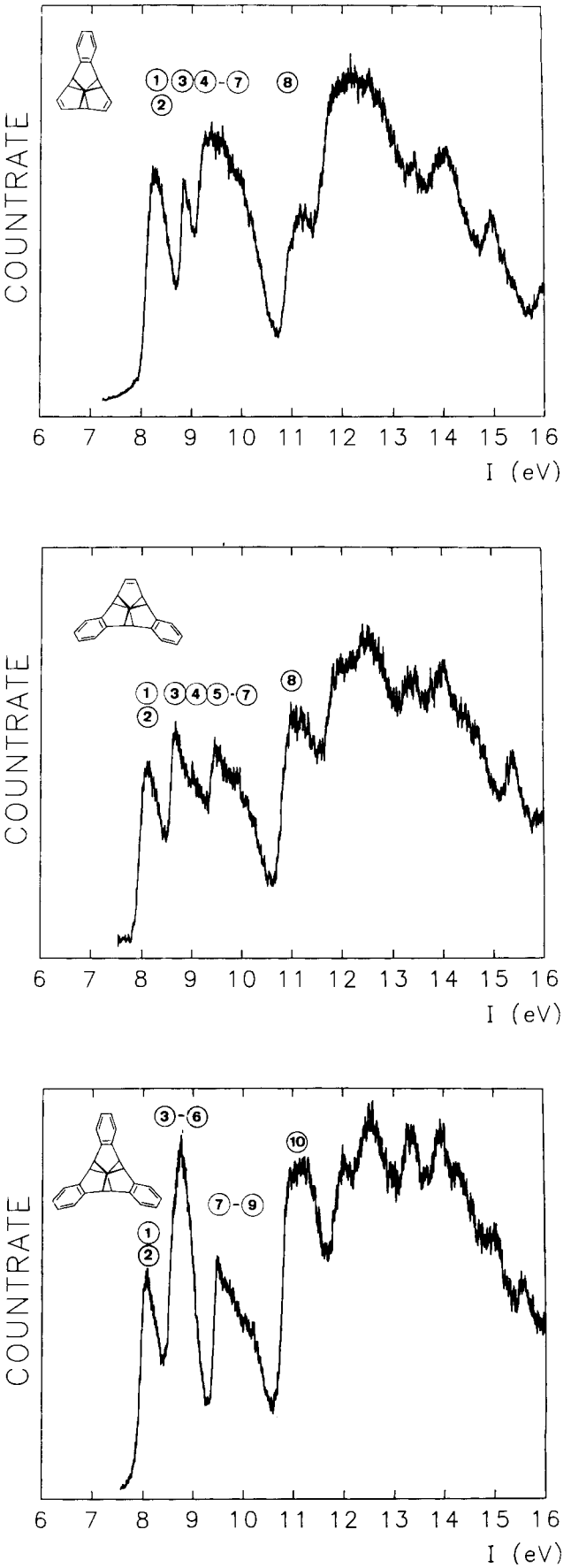

Figure 11. He(I)-PE spectra of **18–20**

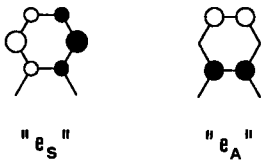

According to a similar first-order treatment[18] the PE spectra of **19** and **20** can be interpreted by adding one or two ethylene π-bands to the PE spectra of **15** and **17**. For the ionization energy of the π-band we estimate a value of ca. 9 eV from the PE spectra of **11** and **12**.

With this assumption we are able to assign the first two peaks in both spectra as ionizations from MOs centered *either at the* benzene ring or at the double bond(s).

Along these lines of reasoning, the broad peak at ca. 10 eV remains for the ribbon orbitals of the triblattane skeleton. MO-calculational results, listed in Table 6, corroborate these qualitative assignments. Furthermore, the calculations suggest that the band at ca. 11 eV in the PE spectra of **19** and **20** should be allocated to the totally symmetric π-MO of the benzene fragments and to a σ-MO at the benzene rings. The splitting between the π-bands in **16**–**18** and **20** is smaller as compared to **6**, **7** and **12**, **13**. This is mainly due to the reduced overlap between the aromatic moieties as compared to the olefinic units. This can be traced back to the smaller AO coefficients at the centers which actually interact.

Table 6. Comparison between the recorded vertical ionization energies, $I_{v,j}$, and the calculated orbital energies, ε_j, of **19** and **20**; all values in eV

Compound	Band	$I_{v,j}$	Assignment[a]	$-\varepsilon_j$ (MNDO/2)
19	1	8.32	21 b(π_B)	9.13
	2		23 a(π_B)	9.26
	3	8.9	22 a(π)	9.59
	4	9.3	20 b(π)	9.98
	5	9.7	21 a(σ_r)	11.05
	6	9.9	29 b(σ_r)	11.12
	7	10.1	20 a(σ_r)	11.48
	8	11.2	18 b(π_B)	12.10
20	1	8.2	27 a(π_B)	9.07
	2		27 b(π_B)	9.17
	3	8.7	26 a(π_B)	9.32
			25 b(π_B)	9.41
	4	9.1	24 b(π)	9.84
	5	9.5	23 b(σ_r)	11.10
	6	to	25 a(σ_r)	11.17
	7	10.0	24 a(σ_r)	11.52
	8	11.1	23 a(π_B)	11.97

[a] π_B = π-MO mainly centered at the benzene rings; σ_r = σ-MO mainly centered at the triblattane skeleton ("ribbon" orbital).

Summary and Conclusions

Our PE investigations of the triblattanes **1**–**4** demonstrate that the ribbon orbitals of the twisted central bicyclo-[2.2.2]octane unit are clearly separated from the remaining σ-MOs. This separation increases with increasing number of ethano bridges, most likely caused by the increasing distortion of the [2.2.2] core. As a consequence of structurally enforced, favorable orbital alignments, triblattanes with exocyclic (**5**–**10**) or endocyclic double bonds display a sizeable splitting of the π-bands. For the two most relevant series of ketones **8**–**10** and endocyclic olefins **11**–**13** the trend and the degree of the OITB effects are graphically summarized in Figure 12. A comparison of the interaction schemes of **7**, **13** and **10** shows that in the first two cases the π-linear combinations e(π) and $a_2(\pi)$ interact with 8e(σ) and $5a_2(\sigma)$ of the [1.1.1]triblattane skeleton (left side of Figure 3). In the case of **10**, however, the interaction takes place with 9e(σ) and $5a_2(\sigma)$. This difference is due to the fact that the wave functions of 9e(σ) are essentially perpendicular to e(π) while the same holds for 8e(σ) and e(n). In comparison with the selected reference 1,4-diketones and 1,5-dienes compiled in Scheme 1, homoconjugation in triketone **10** equals the very favorable situation found in **25**, while that of the triene **13** comes close to that in the structurally related ansaradiene **27**. The effect observed for **13**, however, is clearly smaller than that operative in **28** or **29** because of the close to ideal orbital alignments within the latter[28].

This experimental verification of an efficient through-bond interaction between the π-MOs, as mediated by the

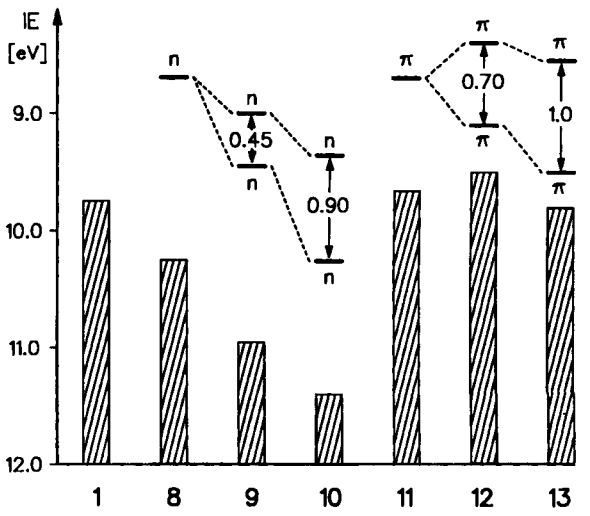

Figure 12. Comparison between the first PE bands of **1** and of the ketones **8**–**10** as well as of the endocyclic olefins **11**–**13**

Scheme 1

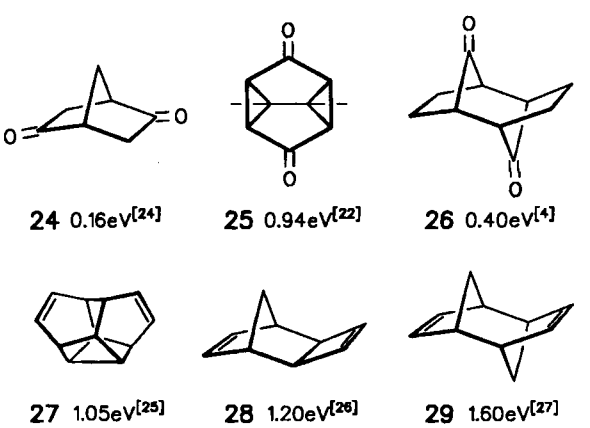

orbitals of these specific σ-frames, is a particularly assertive reward for the expectations which originally had triggered the synthetic conception of these unusual cage compounds[8]. For the benzotriblattanes, on the other hand, the highest occupied MOs are located at the benzene rings between which only relatively small interactions are operative.

We are grateful to *A. Flatow* for recording the PE spectra. We thank the *Deutsche Forschungsgemeinschaft* and the *Fonds der Chemischen Industrie* for financial support.

Experimental

The synthesis of **1**–**20** has been reported[8–11]. The PE spectra of the pure samples were recorded with a Perkin-Elmer PS18 spectrometer equipped with an He(I) light source. Spectra of **1**–**8**, **11**, and **12** were recorded at room temperature, those of the other samples at the following temperatures: **9**: 85°C, **10**: 106°C, **13**: 62°C, **14**: 68°C, **15**: 63°C, **16**: 12°C, **17**: 130°C, **18**: 153°C, **19**: 63°C, **20**: 126°C. The calibration has been carried out with Ar and Xe. A resolution of 20 meV was achieved for the single bands.

[1] R. Gleiter, W. Schäfer, *Acc. Chem. Res.* **1990**, *23*, 369–375.
[2] Reviews: S. Winstein, *Spec. Publ. Chem. Soc.* **1967**, *21*, 5–45. – P. M. Warner, *Topics in Nonbenzenoid Aromatic Chemistry*, Hirokawa Publish Co, Tokyo, **1977**, vol. 2, p. 283. – L. A. Paquette, *Angew. Chem.* **1978**, *90*, 114–125; *Angew. Chem. Int. Ed. Engl.* **1978**, *17*, 106.
[3] H. E. Simmons, T. Fukunaga, *J. Am. Chem. Soc.* **1967**, *89*, 5208–5215; R. Hoffmann, A. Imamura, G. D. Zeiss, *ibid.* **1967**, *89*, 5215–5220. – Review: H. Dürr, R. Gleiter, *Angew. Chem.* **1978**, *90*, 591–601; *Angew. Chem. Int. Ed. Engl.* **1978**, *17*, 559–569.
[4] H.-D. Martin, B. Mayer, *Angew. Chem.* **1983**, *95*, 281–313; *Angew. Chem. Int. Ed. Engl.* **1983**, *22*, 283–314.
[5] D. Elsässer, K. Hassenrück, H.-D. Martin, B. Mayer, G. Lutz, H. Prinzbach, *Chem. Ber.* **1991**, *124*, 2863–2869.
[6] R. Hoffmann, A. Imamura, W. J. Hehre, *J. Am. Chem. Soc.* **1968**, *90*, 1499–1509. – Reviews: R. Hoffmann, *Acc. Chem. Res.* **1971**, *4*, 1–9. – R. Gleiter, *Angew. Chem.* **1974**, 86, 770–775; *Angew. Chem. Int. Ed. Engl.* **1974**, *13*, 696–701. – M. N. Paddon-Row, *Acc. Chem. Res.* **1982**, *15*, 245–251. – M. N. Paddon-Row, K. D. Jordan, *Chem. Rev.* **1992**, *92*, 395–410.
[7] M. R. Wasilewski, *Chem. Rev.* **1992**, *92*, 435–461. – M. A. Fox in *Photoinduced Electron Transfer* (Ed.: M. Chanon), Elsevier, Amsterdam, **1988** and references therein.
[8] W.-D. Fessner, Dissertation, University of Freiburg, **1986**.
[9] H. Müller-Bötticher, W.-D. Fessner, J.-P. Melder, H. Prinzbach, S. Gries, H. Irngartinger, *Chem. Ber.* **1993**, *126*, 2275–2297, preceding paper.
[10] H. Müller-Bötticher, Dissertation, University of Freiburg, **1991**.
[11] W.-D. Fessner, H. Prinzbach, *Tetrahedron* **1986**, *42*, 1797–1803. – H. Müller, J.-P. Melder, W.-D. Fessner, D. Hunkler, H. Fritz, H. Prinzbach, *Angew. Chem.* **1988**, *100*, 1140–1143; *Angew. Chem. Int. Ed. Engl.* **1988**, *27*, 1103–1106. – T. Otten, H. Müller-Bötticher, D. Hunkler, H. Fritz, H. Prinzbach, *Tetrahedron Lett.* **1992**, *33*, 4153–4156.
[12] T. Koopmans, *Physica* **1934**, *1*, 104–113.
[13] M. J. S. Dewar, W. Thiel, *J. Am. Chem. Soc.* **1977**, *99*, 4899–4907, 4907–4917.
[14] P. Bischof, J. A. Hashmall, E. Heilbronner, V. Hornung, *Helv. Chim. Acta* **1969**, *52*, 1745–1749.
[15] E. Heilbronner in *The Chemistry of Alkanes and Cycloalkanes* (Eds.: S. Patai, Z. Rappoport), Wiley, New York **1992**, p. 455–529. – R. Hoffmann, P. D. Mollère, E. Heilbronner, *J. Am. Chem. Soc.* **1973**, *95*, 4860–4862.
[16] C. Sigwart, Dissertation, University of Heidelberg, **1992**.
[17] P. Asmus, M. Klessinger, *Tetrahedron* **1974**, *30*, 2477–2483.
[18] E. Heilbronner, H. Bock, *Das HMO Modell und seine Anwendung*, vol. 1, Verlag Chemie, Weinheim, **1968**. – M. J. S. Dewar, R. C. Dougherty, *The PMO Theory of Organic Chemistry*, Plenum Press, New York, **1975**.
[19] D. Chadwick, D. C. Frost, L. Weiler, *Tetrahedron Lett.* **1971**, 4543–4545.
[20] D. O. Cowan, R. Gleiter, J. A. Hashmall, E. Heilbronner, V. Hornung, *Angew. Chem.* **1971**, *83*, 405–406; *Angew. Chem. Int. Ed. Engl.* **1971**, *10*, 401–489.
[21] G. Jähne, R. Gleiter, *Angew. Chem.* **1983**, *95*, 500–501; *Angew. Chem. Int. Ed. Engl.* **1983**, *22*, 488.
[22] M. Klessinger, *Angew. Chem.* **1972**, *84*, 544–546; *Angew. Chem. Int. Ed. Engl.* **1972**, *11*, 525.
[24] D. C. Frost, N. P. C. Westwood, N. H. Werstiuk, *Can. J. Chem.* **1980**, *58*, 1659–1665.
[25] H.-D. Martin, P. Pföhler, *Angew. Chem.* **1978**, *90*, 901–902; *Angew. Chem. Int. Ed. Engl.* **1978**, *17*, 847.
[26] H.-D. Martin, S. Kagabu, R. Schwesinger, *Chem. Ber.* **1974**, *107*, 3130–3142. – F. Brogli, W. Eberbach, E. Haselbach, E. Heilbronner, V. Hornung, D. M. Lemal, *Helv. Chim. Acta* **1973**, *56*, 1933–1944.
[27] W. Grimme, L. Schumachers, R. Gleiter, K. Gubernator, *Angew. Chem.* **1981**, *93*, 98–99; *Angew. Chem. Int. Ed. Engl.* **1981**, *20*, 113.
[28] For similarly favorable carbonyl/exomethylene interactions see also: A. P. Marchand, C. Huang, R. Kaya, A. D. Baker, E. D. Jemmis, D. A. Dixon, *J. Am. Chem. Soc.* **1987**, *109*, 7095–7101.

[143/93]